



ALTERATION PROCESSES OF HISTORICAL GRANITIC ROCK FOUND IN AVILA, SPAIN

R. García Giménez¹, R. Vigil de la Villa Mencía¹, I. S. de Soto García¹,
J. Caballero Arribas²

¹*Dept. of Geology and Geochemistry. Autonomus University. Madrid. Spain.
C/ Francisco Tomás y Valiente, 7, 28049 Madrid, Spain.*

²*Castellum, archaeologist. Apdo. Correos 396, 05001 Ávila, Spain.*

Received: 17/9/2012

Accepted: 2/3/2013

Corresponding author: García Giménez (rosario.garcia@uam.es)

ABSTRACT

Granitic rock presenting varying alteration processes were sampled from three of five tombs unearthed in Ávila (Spain). The origin of these processes could be both biogenetic and climatic. The purpose of this study is to examine the alteration processes in granitic rocks from the tombs in the area around the Church of San Andrés (Ávila) and to compare these archaeological materials with similar raw materials that could have been employed in their construction. Samples of granitic rock used in the constructive elements of tombs were collected from the same location to compare their physicochemical properties with granite from local quarries. The physical properties of the samples were studied by Polarisation Microscopy and their porosity was determined by BET methodology. Their major and minor constituents were analysed by ICP-MS and their most relevant crystalline mineral compounds (quartz, opal, plagioclase, potassic feldspars, phyllosilicates and hematite) were quantified using X-Ray Diffraction Spectrometry.

KEYWORDS: granitic rock, porosimetry, petrography analysis, alteration, weathering, Spain.

1. INTRODUCTION

Stone is the most abundant of all construction materials used by mankind, however in spite of its great durability and strength, many of its properties are subject to alteration processes (i.e. climatic change, anthropogenic action, flooding).

It is widely accepted that contamination in the form of surface run-off and shallow ground waters in an urban environment with low indices of atmospheric pollution, as well as the long-term effects of mortars, are the most important sources of soluble salts in ornamental stones and the most active factors in any related stone decay.

Stone alteration and weathering processes are determined by natural and anthropogenic factors, which are influenced by various physical, chemical and biological damage parameters (Ariño and Saiz-Jimenez, 1996). The first deterioration process to affect stone begins when it is cut in the quarry and transported to the stonemason's yard, for fashioning as a finished object prior to its final use. Deterioration continues with the exposure of the rock to weathering agents (wind, sunlight, temperature, rain and snow). These agents will induce both physical and chemical weathering processes. A further degradation process is biodeterioration, which follows the initial deteriorating effects of inorganic agents. Changes to the physical parameters of rocks are due to temperature cycles (heating-cooling). This climatic mechanism causes oscillations (periods of expansion and contraction) in the rocks, which produces compressive and tensile stress lines.

The penetration of hyphae into granite rocks usually occurs in the intergranular pores (Wierzchos and Ascaso, 1998) and by cleavage planes in minerals such as biotite, muscovite, and feldspars (Del Monte *et al*, 1996), generating kaolinite (Ascaso, 1985), silica gels (Adamo *et al*, 1993), oxalates, carbonates and sulfates (Edwards and

Seaward, 1995), as well as iron oxides (Gehrmann and Krumbein, 1994). Many of the aforementioned compounds were present in the samples taken from the tombs.

Heating-cooling cycles take place with the highest frequency on the south and the west sides of the tombs during summer. The temperature cycles produce a thermal gradient within the rocks leading to thermal stress or insolation weathering. Differences in the rate of thermal expansion between superficially degraded minerals or stone may also contribute to the breakdown of the rock.

The most likely explanation is that the daily variation of the atmospheric temperature dynamically drives the fluid flow from inside the rock towards its surface where the water evaporates. The process of mineral dissolution, transport and subsequent recrystallization, the result of temperature driven fluid flows, can for example cause continuous delamination of sandstone surfaces.

Previous studies have considered the relation between dissolution rates and neoformed minerals such as kaolinite, albite, and smectite (Oelkers and Schott, 1999; Taylor *et al*, 2000; Berger *et al*, 2002). Silva *et al* (1997) demonstrated the importance of roughness and porosity in the alteration processes of granite and took account of secondary processes due to the high degree of weathering of the granite in their study. As water is a limiting factor, physical properties related to the processes of intake, loss and movement of water inside the rock were also measured: the kinetics of wetting and drying; the maximum amount of water absorbed under vacuum (water saturation); the degree of saturation, (i.e., the relation, expressed as a percentage, between the maximum amount of freely absorbed water and the maximum amount of water absorbed under vacuum); the maximum amount of water absorbed by capillarity suction (capillary water content);

and the capillarity coefficient that indicates the speed of capillary suction (Prieto and Silva, 2005).

These alteration processes are conditioned by the origin of materials, the orientation of the construction, and may even depend on the microenvironmental conditions of the zones in which they are located. All these factors mean that the evolution of different areas of the stone will vary: basal zones subjected to salt-loaded humidity due to capillary ascent; high zones with filtering, leading to alteration accompanied by the washing out of elements and material loss; vertical surfaces, less affected by weathering and the mobility of the different chemical elements, associated with the dominant weathering process in each case.

The purpose of this study is to examine the alteration processes in granitic rocks from the tombs in the area around the Church of San Andrés (Ávila) and to compare these archaeological materials with similar raw materials that could have been employed in their construction.

2. MATERIALS AND METHODS

2.1 Materials

The city of Avila is situated in the interior of the Iberian Peninsula (40°39'N-4°44'30'W), on a granite platform at an altitude of 1,100-1,200 m a.s.l. It has a Mediterranean climate with a continental trend and its atmosphere shows low pollution indices, below the detection limit of the measuring systems of the J.C.L. Environmental Health Office mobile unit. The area has a mean annual precipitation of 370 mm, with a mean relative atmospheric humidity of 57% and an annual temperature that fluctuates between 36.8°C and -16°C. On average, there are 210 days with minimum mean temperatures of below 0 °C each year. All of this points to sharp hydric and thermal changes that generate strong surface tensions on the

building materials.

Excavations in the area surrounding the Church of San Andrés have unearthed five tombs in different states of conservation, with very different chronologies (Fig.1 and 2). The most ancient of the five tombs, at the Romanic level, was sealed at a very early point, around the end of the 12 c. All the tombs consist of graves with uncouth caleño granite flagstones on the floors and even on some of the walls (Fig. 1 A and B).



Figure 1. Location map and San Andrés Church image. A) and B) Detail of the tombs.

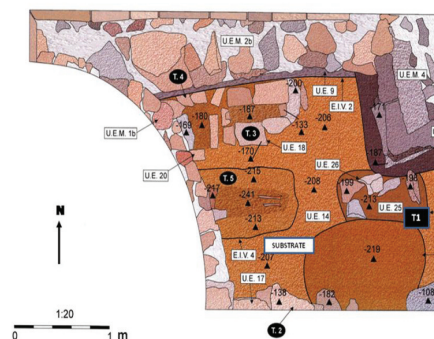


Figure 2. Schematic arrangement of the studied units (tombs 1, 2, 3, 4 and 5).

Samples of materials from both the exterior and the interior of the Church of San Andrés were taken at different weathering levels and from various zones exposed to different environments (lower parts of walls affected by humidity by capillary rise, undeteriorated intermediate zones, columns and values affected by

filtrations from roofs and terraces).

These types of tombs, though, generally, of a greater height and with more carefully worked head-boards, have been well dated and documented in other necropolis around the old town of Ávila and the San Vicente basilica (UNESCO World Heritage site) (Caballero Arribas, 1996).

The highly altered state of the granitic rocks from the tombs has prompted this study on their weathering processes and a study of the materials from nearby quarries that could have been used in their construction. Clean rocks were sought, similar to the rock supplied by constructors (for restoration work) from quarries near Ávila, in order to study the origins of the alteration processes.

The first step was to locate sources for the supply of comparable materials, which were eventually found near the city of Avila (La Colilla, Las Hálagas, El Lomo) (García Talegón *et al*, 1999), where the exploitation of these types of granite rocks continues for restoration purposes and as a source of ornamental stone, known as ochre granite or *caleño*, as well as silcrete, another granite known as bleeding stone (*Sangrante*).

Three granite rock samples were taken from the five tombs (1, 2, 3, 4 and 5) and two further samples from the quarry environment: "*caleño*" granite and bleeding stone.

2.2 Methods

Mineralogical composition was studied by X-ray diffraction (XRD), using the random powder method for the bulk sample, and the oriented slides method for the <2 μm fraction. A SIEMENS D-500 X-ray diffractometer equipped with a Cu anode, operated at 30 mA and 40 kV using divergence and reception slits of 2 and 0.6 mm, respectively. The XRD profiles were measured in 0.04 2θ goniometer steps for 3s.

Textural and morphological character-

izations were performed by using a SEM-EDAX device (PHILIPS XL30, W source, DX4i analyser and Si/Li detector). The analyzer was previously calibrated with a multimineral sample: the USGS standard ADV-1 (Govindaraju, 1994).

Transversal thin sections (20-25 μm) were cut off the samples, in order to observe several components in a Petrographic Polarisation Orto Plan Pol Leitz Microscope. When suitably thin sections of the samples were not easily available, the samples were consolidated with resin and the sections were cut off, following drying, as previously described.

Following the dissolution of each sample, the content of Al_2O_3 , CaO , MgO , K_2O , Na_2O , Fe_2O_2 , MnO , and TiO_2 were determined as major constituents, and SiO_2 was determined by difference. These chemical elements were calculated by inductively coupled plasma-mass spectrometry (ICP-MS, Perkin-Elmer Sciex Elan 6000 equipped with an AS 91 autosampler). Moreover, blank samples, standard samples and duplicated samples were simultaneously performed as quality control.

Specific surface area study, N_2 BET surface, was determined in a GEMINI V micrometrics porosimeter after degassing under N_2 flow for 18 h at 90°C. The BET surface area provided information on the outer surface of the sample aggregates. A method developed by Brunauer *et al.* (1938) was used for determination, based on physical adsorption of gases at temperatures close to their condensation temperature, considering the isotherms of nitrogen adsorption /desorption.

3. RESULTS AND DISCUSSION

The sample of ochre granite or *caleño* was identical to the samples from the Las Hálagas and El Lomo quarries. They were all formed from tropical weathering processes, but the *caleño* sample differed

with regard to variations in its own petrophysical characteristics (García Talegón *et al*, 1999). Other granite rocks such as bleeding stone and silcrete originated from a silicification process of the opal CT, with kaolinitization processes, remobilisation of iron oxyhydroxides and silicification by opal CT. This is a SiO₂ variety of fibrous structures formed through bacterial action (Bustillo, 1995). The samples from the tombs are granitic rock that have been completely transformed into sand.

3.1. Mineralogical study

Petrographic studies revealed that the granitic rocks from the tombs contained very fragile altered feldspars. The mineralogical composition of the samples from the tombs analysed by XRD was quartz, feldspar (Fig. 3 and Table 1), opal, hematite, kaolinite, illite and smectite. Quartz and feldspars are the minerals with the largest presence in the samples (Fig. 4A and 5B). Quartz crystals showed allotriomorphic forms and sometimes polycrystalline aggregates. The potassium feldspar was orthoclase, usually with inclusions of other minerals such as biotite, quartz, and plagioclase. Most of the plagioclases were oligoclase; occasionally with intracrystalline microfissures and slight seritization of the nuclei (Fig. 4B). Muscovite was only present as an accessory mineral, together with zircon and opaque minerals. Bleeding stone or *sangrante* is a highly altered granite with clay minerals and opal granite that is rich in hematite (Fig. 4C). The morphology of the minerals from the tombs is thoroughly different: it presents abundant pores (Fig. 4C) and the feldspars have been transformed into clay minerals (Fig. 4D and 5C).

Sample	Quartz (%)	K Feldspar (%)	Ca/Na Feldspar (%)	Opal (%)	Kaolinite (%)	Illite (%)	Smectite (%)	Hematite (%)	Micas (%)
"Caleño" granite	25	traces	traces	30	36	n.d.	2	5	2
3	10	traces	n.d.	20	50	n.d.	20	1	n.d.
Bleeding stone	18	29	23	n.d.	n.d.	25	n.d.	n.d.	5
4	13	32	20	n.d.	10	25	n.d.	n.d.	n.d.
5	13	28	14	n.d.	15	30	traces	n.d.	n.d.

Table 1. Mineralogical composition of the samples (n.d. = not detected).

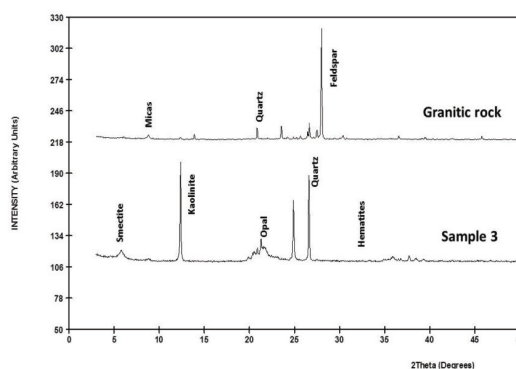


Figure 3. XRD patterns of the tomb 3 and granitic rock.

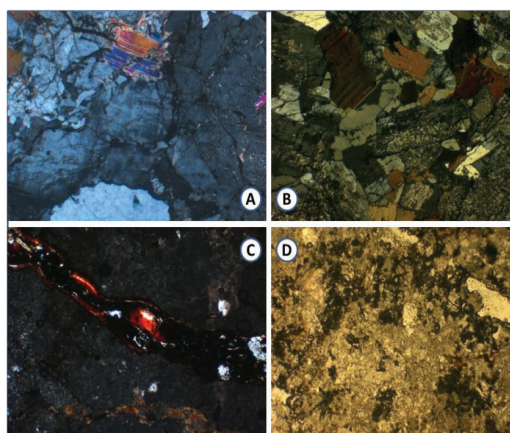


Figure 4. Petrographic studies: A) Large feldspar crystal from "caleño" granite (X64 crossed nicols). B) Detail of biotite and feldspar seritized crystals from "caleño" granite (X64 crossed nicols). C) Hematite crystal from the bleeding stone (X64 crossed nicols). D) Altered minerals to clay minerals from the tomb 3 (X64).

Degradation of feldspars and micas took place due to the weathering processes (Churchman and Gilkes, 1989; Bjorkum *et al*, 1990) (Fig. 5F). In general, it was

considered that the kaolinite present in the original materials was a product of previous mineralogical alterations. The high kaolinitization process in the caleño granite (Fig. 5A) produced a highly unstable, fragile and easy to work material, which meant that some blocks were sculpted into anthropomorphic forms. The mobilized silica crystallized as opal spheres that are preserved in the material (Fig. 5E).

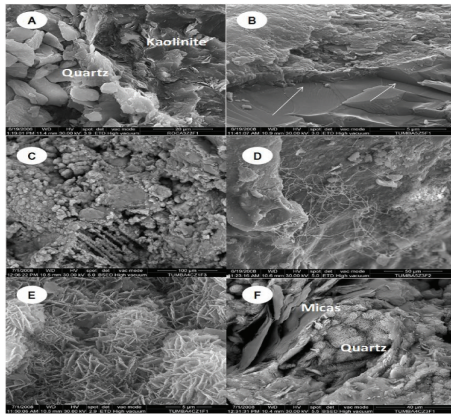


Figure 5. SEM microscopy: A) Detail of quartz and kaolinite in the "caleño" granite from Las Hálagas quarry. B) Alteration front into feldspar crystal to the "caleño" granite. C) Altered feldspar from the tomb 3. D) Hyphae in material rock from tomb 5. E) Opal spheres from tomb 4. F) Quartz and micas from tomb 4.

Feldspar alteration processes shows etch pit morphologies in SEM imaging, revealing rhombus-shaped, crystallographically controlled etch pits on all samples. Both pyramidal and flat-bottomed etch pits were present (Beig and Lüttge, 2006). According to accepted theory, etch

pits form where, for example, line defects, such as screw dislocations that originate within the crystal lattice intersect its surface. These dislocations are identified dissolution fronts continuing the growth steps of the feldspar (Fig. 5B and 5C). Dissolving mineral surfaces are the mechanisms (Casey and Ludwig, 1995) that explain the decrease of silica content in the compositions in relation to the tombs (Table 2).

Table 1 shows the mineralogical analysis. The materials from tomb 3 are similar to the sample "caleño" granite: there are kaolinite, quartz, opal, hematite and smectite. In comparison with the "caleño" granite, the tomb material shows a major alteration: its kaolinite and smectite contents are higher than in the original rock. The material from tombs 4 and 5 are similar to the bleeding stone from the El Lomo quarry.

Biodegradation processes were identified by the presence of hyphae in tomb 5 (Fig. 5D) which contribute to feldspar alteration and its transformation into clay minerals (Mansch and Bock, 1993).

3.2. Specific surface area study

Considering the granitic nature of the samples (Table 2), they present a high level of porosity (near values of 17%), mainly represented in families of microporosity (93%) (not recognized in the petrographic microscope), which are largely of the trapped type. In addition, there is a significant percentage of fissural type porosity identified by SEM near feldspars

Sample	SiO ₂	Al ₂ O ₃	CaO	MgO	Na ₂ O	K ₂ O	Fe ₂ O ₃	MnO	TiO ₂
"Caleño" granite	65.58	9.70	6.40	3.20	8.57	2.25	2.57	0.04	1.69
3	40.83	32.77	4.65	3.95	6.60	7.96	1.58	0.03	1.63
Bleeding stone	46.62	15.59	9.74	4.36	12.11	2.04	7.53	0.05	1.96
4	32.30	32.84	8.73	4.61	9.29	2.59	6.79	0.04	2.81
5	40.00	26.50	5.77	3.99	7.33	7.99	6.37	0.05	2.00

Table 2. Chemical analyses of the major elements in %.

which originated from their alteration processes. In general, high porosity is shown and the degree of alteration increases as the grain size is reduced (Vigil de la Villa *et al.*, 2000).

The most porous material was found in tomb 3 (Table 3). However, the sample from tomb 3 was similar to *caleño* granite, as the alteration processes of the stone left buried under the soil lead to high porosity values. Bulk density and open porosity are related to the consistency of the rock; open porosity reflects the volume of empty pores interconnected to each other and to the exterior. It is therefore important, due to the movement and storage of water in a rock, and consequently to the bioreceptivity of the rock. Both water saturation and capillary matter followed the same order, in terms of porosity (Zouridakis and Tzevelekos, 1999).

Sample	Specific surface BET (m ² /g)
"Caleño" granite	16.87
3	22.15
Bleeding stone	7.99
4	18.12
5	17.22

Table 3. BET Specific Surface Area (m²/g) of the samples

3.3. Chemical analysis study

Chemical analysis of the major elements (Table 3) and reference to petrographical criteria allows us to associate the sample from tomb 3 with "*caleño*" granite. Bleeding stone has greater affinity to the material from tombs 4 and 5. These results are consistent with those described in the XRD technique.

The alteration process of the tomb materials is evident in the decrease of the silica content that is compensated by the increase in the alumina content. Weathering

affects the silica, CaO, Na₂O and Fe₂O₃ content. In tomb 3, the loss of silica is close to 40%.

Analysis of the minor elements (Table 4) provides a large volume of comparative data that supports the association of the material from tomb 3 with the "*caleño*" granite and the material from tombs 4 and 5 with bleeding stone. The elements that allow us to affirm those similarities are P, Sc, Ni, Cu, Zn and Rb.

It is worth mentioning the high content of boron and barium and the minor concentrations of neodymium and lead in the original granitic rocks from the tombs when compared to the raw material from the quarries. Washing processes in the granitic rocks from the tombs and the exchange with the environment are responsible for the assimilation of some and the reduction of other elements.

4. CONCLUSIONS

The granitic rock employed in the construction of flagstones in the tombs found around the Church of San Andrés is closely comparable to different types of rock sampled from a nearby quarry front. The assumption that granitic rocks were quarried in the local environment has previously been suggested (Caballero Arribas, 1996; García Talegón *et al.*, 1999), although these studies were not conducted with the same techniques and at the same archaeological site as this study

XRD analysis has indicated the link between the quarry samples and the tomb samples. The materials from tomb 3 are similar to the sample "*caleño*" granite: kaolinite, quartz, opal, hematite and smectite are all present, but the granite rock from the tomb is greatly altered by weathering, while the bleeding stone forms part of tombs 4 and 5. The other two tombs, numbers 1 and 2, present a different lithology from the above mixture.

Atmospheric agents affect the stability of

Sample	Li	B	P	Sc	Cr	Ni	Cu	Zn	Ga	Rb	Sr	Y	Zr	Nb	Sn	Cs	Ba	La	Ce	Pr	Nd	Sm	Gd	Pb
"Caleño" Granite	9	n.d.	57	3	n.d.	15	21	17	9	9	15	11	19	4	14	1	63	33	91	13	55	10	8	496
3	46	339	26	4	6	5	13	12	18	43	166	23	102	12	4	2	43	47	98	11	39	11	7	50
Bleeding stone	25	40	434	14	11	24	35	147	14	102	10	84	60	7	7	3	137	135	284	37	144	29	27	87
4	43	240	480	13	27	30	39	125	17	115	n.d.	21	50	9	1	7	629	23	46	7	28	6	6	23
5	50	328	422	15	37	46	44	137	20	123	n.d.	26	61	12	n.d.	10	157	28	51	9	25	9	8	33

Table 4. Chemical analyses of the minor elements in $\mu\text{gg-1}$ (n.d. = not detected)

the rocks counterfoil, stimulating the alteration and the creation of new minerals. Washing processes have increased due to the contribution of hyphae.

The degree of alteration was found to increase as the grain size decreased and the samples were very much more porous than the raw granitic rock samples. This fact facilitates weathering and assists the processes of dissolution and neof ormation.

Analysis of the tombs has shown that the granitic rocks in each tomb were not from the same quarry and that some rock fragments have possibly been reused. However, the comparison with samples taken from two nearby quarries adds weight to the assumption that they came from the same area, taking into account the presence of several granite fronts of similar lithology.

REFERENCES

- Adamo, P., Marchetiello, A., Violante, P., (1993), The weathering of mafic rocks by lichens, *Lichenologist*, 25(3): 285-297.
- Ariño, X. and Saiz-Jimenez, C., (1996), Factors affecting the colonization and distribution of cyanobacteria, algae and lichens in ancient mortars, in: J. Riederer J (ed.), *Proceedings of the Eighth International Congress on Deterioration and Conservation of Stone*, vol. 2, Rathgen-Forschungslabor, Berlin, Germany, pp. 724-731.
- Ascaso, C., (1985), Structural aspects of lichens invading their substrata, in: C. Vicente, D.H. Brown, E. Legaz (Eds.) *Surface Physiology of Lichens*, Universidad Complutense. Madrid, Spain, pp. 87-113.
- Beig, M.S. and Lüttge, A., (2006), Albite dissolution kinetics as a function of distance from equilibrium: Implications for natural feldspar weathering, *Geochimica and Cosmochimica Acta*, 70, 1402-1420.
- Berger, G., Beaufort, D., Lacharpagne, J.L., (2002), Experimental dissolution of sanidine under hydrothermal conditions: mechanism and rate, *American Journal Science*, 302:663-685.
- Bjorkum, P.A., Mjos, R., Walderhaug, O., Hurst, A., (1990), The role of the alteration Cimmerian uncorformity for the distribution of kaolinite in the Gullkaks Field, northern North Sea, *Sedimentology*, 7, 395-406.
- Brunauer, S., Emmet, P.H., Teller, E., (1938), Adsorption of gases in multimolecular layers, *Journal of the American Chemical Society*, 60 (2), 309-319.
- Bustillo, M.A., (1995), Una nueva ultraestructura de ópalo CT en silcretas. Posible indicador de una influencia bacteriana, *Estudios Geológicos*, 51, 3-8.
- Caballero Arribas, J., (1996), La plaza de San Vicente de Ávila: necrópolis parroquial y

- nivel romano, *Numantia*, 6:128-132.
- Casey, W.H. and Ludwig, C. (1995), Silicate mineral dissolution as a ligand-exchange reaction, in: A.F. White, S.L. Brantley (eds.), *Chemical weathering rates of silicate minerals*, Min. Soc. Am., Washington, USA 31, pp. 87-118.
- Churchman, G.J. and Gilkes, R.J., (1989), Recognition of intermediates in the possible transformation of halloysite to kaolinite in weathering profiles, *Clay Minerals*, 24: 579-590.
- Del Monte, M., Rattazi, A., Romao, P.M.S., Rossi, P., (1996). The role of lichens in the weathering of granitic buildings, in: M.A. Vicente, J. Delgado Rodrigues, J. Acevedo (Eds.) *Proceedings of Workshop on Degradation and Conservation of Granitic Rocks*, Santiago de Compostela, Spain, pp. 301-306.
- Edwards, H.G.M. and Seaward, M.R.D., (1995), FT-Raman spectroscopic studies of lichen-substratum interfaces in biodeterioration studies, *Biodeterioration and Biodegradation*, 9:199-203.
- García Talegón, J., Vicente, M.A., Molina-Ballesteros, E., Vicente-Tavera, S., (1999), Determination of the origin and evolution of building stones as a function of their chemical composition using the inertia criterion based on an HJ-biplot, *Chemical Geology*, 153: 37-51.
- Gehrmann, C. and Krumbein, W.E., (1994), Interactions between epilithic and endolithic lichens and carbonate rocks, in: V. Fassina, H. Ott, F. Zezza (Eds.) *Proceedings of the 3er International Symposium The Conservation of Monuments in the Mediterranean Basin*. Venecia, pp. 311-316.
- Govindaraju, K., (1994), *Compilation of working values and samples description for 383 geostandards*, Geostandards Newsletter special issue. Vandoeuvre, Lès Nancy, France, vol. XVIII, 158 pp.
- Mansch, R, Bock, E., (1993), Untersuchung der Beständigkeit von keramischen, *Werkstoffe Korrosion*, 45:96-104.
- Oelkers, E.H. and Schott, J., (1999), Experimental study of kyanite dissolution rates as a function of chemical affinity and solution composition, *Geochimica and Cosmochimica Acta*, 63 (6):785-797.
- Prieto, B. and Silva, B., (2005), Estimation of the potential bioreceptivity of granitic rocks from their intrinsic properties, *International Biodeterioration and Biodegradation*, 56:206-215.
- Silva, B., Prieto, B., Rivas, T., Sánchez Biezma, M.J., Paz, G., Carballal, R., (1997), Rapid biological colonization of a granitic building by lichens, *International Biodeterioration and Biodegradation*, 40:263-267.
- Taylor, A.S., Blum, J.D., Lasaga, A., (2000), The dependence of labradorite dissolution and Sr isotope release rates on solution saturation state, *Geochimica and Cosmochimica Acta*, 64: 2389-2400.
- Vigil de la Villa, R., García, R., Rubio, V., Ballesta, R.J., (2000), Soil alteration processes on granite in the Central Mountain Range (Spain), *Z. Geomorphology*, 44(2): 233-248.
- Wierzchos, J. and Ascaso, C., (1998), Mineralogical transformation of bioweathered granitic biotite, studied by HRTEM evidence for a new pathway in lichen activity, *Clays and Clay Mineralogist*, 46(4): 446-452.
- Zouridakis, N. and Tzevelekos, K., (1999). Nitrogen porosimetry on ancient ceramics, *Journal European Ceramic Society*, 19:89-92.